AIP | The Journal of Chemical Physics

Electronic transitions of palladium dimer

Yue Qian, Y. W. Ng, Zhihua Chen, and A. S.-C. Cheung

Citation: The Journal of Chemical Physics **139**, 194303 (2013); doi: 10.1063/1.4829767
View online: http://dx.doi.org/10.1063/1.4829767
View Table of Contents: http://scitation.aip.org/content/aip/journal/jcp/139/19?ver=pdfcov
Published by the AIP Publishing

Electronic transitions of palladium dimer

Yue Qian, Y. W. Ng, Zhihua Chen, and A. S.-C. Cheung[a)]
Department of Chemistry, The University of Hong Kong, Pokfulam Road, Hong Kong

(Received 9 July 2013; accepted 28 October 2013; published online 15 November 2013)

The laser induced fluorescence spectrum of palladium dimer (Pd_2) in the visible region between 480 and 700 nm has been observed and analyzed. The gas-phase Pd_2 molecule was produced by laser ablation of palladium metal rod. Eleven vibrational bands were observed and assigned to the $[17.1]^3\Pi_g - X^3\Sigma_u^+$ transition system. The bond length (r_o) and vibrational frequency ($\Delta G_{1/2}$) of the ground $X^3\Sigma_u^+$ state were determined to be 2.47(4) Å and 211.4(5) cm^{-1}, respectively. A molecular orbital energy level diagram was used to understand the observed ground and excited electronic states. This is the first gas-phase experimental investigation of the electronic transitions of Pd_2.
 [http://dx.doi.org/10.1063/1.4829767]

I. INTRODUCTION

Palladium (Pd) is an interesting transition metal. The metal itself is an active catalyst, many palladium-containing compounds such as palladium acetate,[1] palladium nanoparticles,[2] and palladium alloys[3] also have catalytic properties. Palladium-catalyzed coupling reactions, such as in the formation of carbon-carbon bonds, are extremely useful in organic synthesis.[4] Many complex reactions involving Pd are well known, but simple diatomic molecules that can provide fundamental knowledge of the metal bonding are amongst the least studied. For diatomic molecules formed from Pd and the first row main group elements, preliminary work has only been reported for PdC,[5,6] PdO,[7] and PdB[8] molecules; however, nothing is experimentally known for the PdN and PdF molecules.

Palladium dimer (Pd_2) is an excellent starting point for studying the properties of Pd metal bonding. There have been many theoretical calculations concerning the ground and low-lying electronic states of Pd_2.[9–27] Shim and Gingerich conducted non-relativistic all electron *ab initio* Hartree Fock (HF) with configuration interaction (CI) calculation, and predicted a $^1\Sigma_g^+$ ground state with a bond length of 2.75 Å.[11] Balasubramanian, using CASSCF/MCSCF followed by multireference single and double CI, and relativistic CI calculations,[13,14] calculated 41 low-lying electronic states and predicted the ground state to be a $^3\Sigma_u^+$ state. Almost simultaneously, Kleinman and co-workers used local-spin-density (LSD) theory calculations also obtained a $^3\Sigma_u^+$ ground state.[15] Subsequently, both Schwerdtfeger *et al.*[16] who employed a size-consistency-corrected CI method with electron correlation effects and Zerner *et al.*[17] who used the SCF/CI level obtained a $^3\Sigma_u^+$ ground state. Harada and Dexpert,[19] and Efremenko *et al.*[23] used different density functional theory (DFT) methods, both obtained triplet ground state for Pd_2. Experimental investigation has proven to be a challenging and difficult task. Pd_2 was first studied by Ozin *et al.*[28] in noble gas matrices. The absorption spectrum was recorded and a weak transition in the UV region was attributed to Pd_2 species, but no detailed analysis was made. The Morse group[29] has attempted to record the spectrum of Pd_2 in the visible and near IR regions using two-photon ionization spectroscopy, but no transition was observed. Lineberger and co-workers,[30,31] using photo-detachment spectroscopy, studied several low-lying electronic states and determined the ground state of Pd_2 to be the $X^3\Sigma_u^+$ state.

In this work, we report the $[17.1]^3\Pi_g - X^3\Sigma_u^+$ transition system of Pd_2 in the visible region. The ground $X^3\Sigma_u^+$ state has been confirmed and an accurate vibrational frequency was determined. The spin splitting of the ground state has been discussed and a molecular orbital (MO) energy level diagram is used to understand the electronic structure of the Pd_2 molecule. Our obtained results are also compared with the Group VIIIA and IB transition metal dimers.

II. EXPERIMENT

The apparatus used for obtaining the LIF spectrum of Pd_2 has been described in previous publications.[32,33] A brief description of the relevant experimental conditions is given here. The Pd_2 spectrum was first observed when we studied the spectrum of PdB molecule[8] by reacting laser ablated Pd atoms with 0.5% diborane (B_2H_6) seeded in argon. The Pd_2 spectrum could also be recorded with the Pd_2 molecule produced from laser ablation of a Pd rod in the presence of pure argon, but the signal-to-noise ratio of the spectrum was worse. Subsequently, all Pd_2 spectra were recorded with the presence of a trace amount of diborane in argon. Both tunable pulsed dye and optical parametric oscillator (OPO) lasers were used to excite the Pd_2 molecule. They were individually pumped by different Nd:YAG lasers with wavelength set to 355 nm, giving tunable output wavelength covering the UV and visible regions. The energy output from the tunable pulsed lasers was about 10 mJ/pulse, the wavelength of the lasers was measured by a wavelength meter with accuracy around ±0.02 cm^{-1}, and the linewidth of the dye and OPO lasers was found to be about 0.07 and 0.12 cm^{-1}, respectively. The tunable laser output was used to excite the

a)Author to whom correspondence should be addressed. Electronic mail: hrsccsc@hku.hk. Tel.: (852) 2859 2155. Fax: (852) 2857 1586.

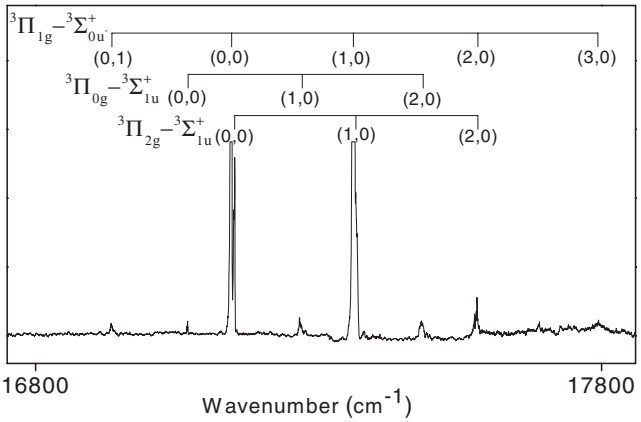

FIG. 1. LIF spectrum of Pd_2 with sub-band assignment (see text).

jet cooled Pd_2 molecule. The LIF signal was directed into a 0.30 m monochromator and it was subsequently detected by a photomultiplier tube (PMT) at the exit slit of the monochromator. The monochromator was used for two purposes: (i) obtaining wavelength resolved fluorescence spectrum and (ii) as an optical filter in recording the LIF spectrum. The PMT output was fed into a fast oscilloscope for averaging and storage.

III. RESULTS AND DISCUSSION

The LIF spectrum of Pd_2 in the region between 480 nm and 700 nm was studied. Eleven vibrational bands were recorded and analyzed. Figure 1 depicts the LIF spectrum of Pd_2 with three sub-band transitions identified and labeled. The (0, 0) and (1, 0) bands have large intensity and were truncated to enhance the weaker transition bands shown in the diagram. The wavelength resolved fluorescence spectrum of the (0, 0) band of the $^3\Pi_{1g} - {}^3\Sigma^+_{0u^-}$ transition at 583.2 nm is given in Figure 2, which shows clearly a vibrational sequence with separation about 210 cm^{-1}. This vibrational separation matches well with the value obtained by Lineberger and his co-workers,[30,31] and is consistent with the

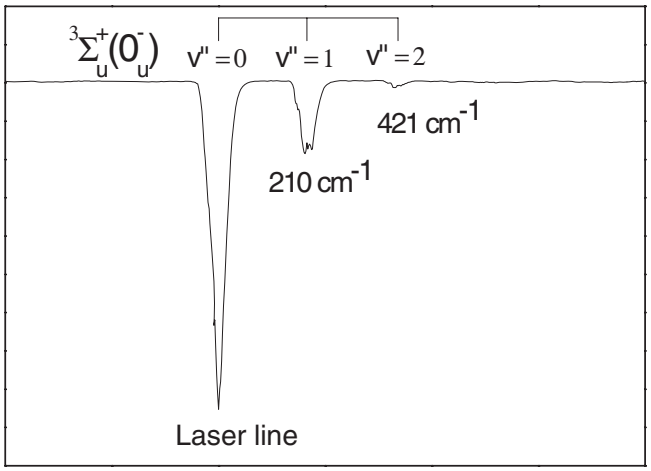

FIG. 2. Wavelength resolved fluorescence spectrum of the (0, 0) band of the $^3\Pi_{1g} - {}^3\Sigma^+_{0u^-}$ sub-band transition of Pd_2.

carrier of the spectrum being Pd_2. In addition, these bands are very congested and have no resolved rotational structure. The palladium atom has six naturally occurring isotopes and five of them have relatively large natural abundances [^{104}Pd (11.14%), ^{105}Pd (22.33%), ^{106}Pd (27.33%), ^{108}Pd (26.46%), ^{110}Pd (11.72%)]. For the palladium dimer, there are a total of 15 isotopic molecules that can be formed from these atoms and they all have sizable contributions to the observed band. These isotopic molecules have slightly different reduced masses, hence, slightly different vibrational and rotational constants, and the observed band shows no resolved rotational structure but only heavily overlapped band structure. The observed bands have been assigned to be the $[17.1]^3\Pi_g - X^3\Sigma^+_u$ transition system of Pd_2. In addition to the visible region, the UV region has also been searched for possible Pd_2 transition. Ozin *et al.*[28] studied palladium atoms and molecules isolated in solid argon, a weak absorption transition at 265 nm was attributed to the Pd_2 molecule. We have searched extensively for this weak absorption band in this work; however, no transition could be found in this spectral region.

For the ground $X^3\Sigma^+_u$ state, a broadening of the band in the photo-detachment spectrum by about 30 cm^{-1} was interpreted as likely to be arising from the splitting into $\Omega = 0_u^-$ and $\Omega = 1_u$ components by Lineberger *et al.*[30,31] This splitting was calculated by Balasubramanian[13] to be 9 cm^{-1}, with the $\Omega = 1_u$ component lying lower in energy. This splitting arises from second-order spin-orbit coupling effects, which become significant in heavier transition metals such as palladium. As far as the upper state is concerned, the observed band system shows one intense set of sub-bands and two other much weaker sets of sub-bands. When the $X^3\Sigma^+_u$ state is the lower state, the only electric-dipole allowed transitions that can give such results are namely, $^3\Pi_{2g} - {}^3\Sigma^+_{1u}$, $^3\Pi_{1g} - {}^3\Sigma^+_{0u^-}$, $^3\Pi_{0g} - {}^3\Sigma^+_{1u}$, where it is assumed that the Λ-type doubling between the $\Omega = 0$ components of the $^3\Pi_g$ state is too small to be resolved. Furthermore, if the $^3\Sigma^+_u$ spin splitting is large, with the $^3\Sigma^+_{0u^-}$ level lying lower in energy, then a low thermal population in the $^3\Sigma^+_{1u}$ level can explain the weak intensity of the $^3\Pi_{2g} - {}^3\Sigma^+_{1u}$ and $^3\Pi_{0g} - {}^3\Sigma^+_{1u}$ sub-bands. Accordingly, the bands with the largest intensity have been assigned to be the (0, 0) and (1, 0) band of the $^3\Pi_{1g} - {}^3\Sigma^+_{0u^-}$ ($\Omega = 1 - \Omega = 0$) sub-band and a clear v′-progression can be observed in this sub-band. The two lower intensity band sequences have been assigned as $^3\Pi_{0g} - {}^3\Sigma^+_{1u}$ ($\Omega = 0 - \Omega = 1$) and $^3\Pi_{2g} - {}^3\Sigma^+_{1u}$ ($\Omega = 2 - \Omega = 1$) sub-bands. While the $^3\Pi_{0g} - {}^3\Sigma^+_{1u}$ sub-band is well separated in energy, the $^3\Pi_{2g} - {}^3\Sigma^+_{1u}$ sub-band gradually overlaps with the $^3\Pi_{1g} - {}^3\Sigma^+_{0u^-}$ group as the v′ number increases, especially in the case of (1, 0) band and (2, 0) bands. Under this assignment, the two sets of sub-bands with $\Delta\Omega = +1$ are of larger intensity than the one with $\Delta\Omega = -1$. This is consistent with the situation that the transition strength of sub-bands with $\Delta\Omega = +1$ is larger for a $\Delta\Lambda = +1$ transition. Since the $^3\Pi_{2g} - {}^3\Sigma^+_{1u}$ sub-band is higher in energy than the $^3\Pi_{0g} - {}^3\Sigma^+_{1u}$ sub-band, the upper state has been assigned as a regular $^3\Pi_g$ state with the $\Omega = 2$ sub-state higher in energy in this work. However, our assignment was based only on intensity consideration; there might still be slight possibility that

TABLE I. Observed band origin for the $[17.1]^3\Pi_g - X^3\Sigma_u^+$ transition of Pd_2 (cm^{-1}).

Sub-band transition	Vibrational band (0, 1)	(0, 0)	(1, 0)	(2, 0)	(3, 0)
$^3\Pi_{2g} - {}^3\Sigma_{1u}^+$		17 151.7	17 368.9	17 581.5	
$^3\Pi_{1g} - {}^3\Sigma_{0u^-}^+$	16 934.9	17 146.3	17 364.4	17 581.5	17 796.4
$^3\Pi_{0g} - {}^3\Sigma_{1u}^+$		17 069.7	17 271.2	17 484.8	

TABLE II. Molecular constants used to obtain the band contour of the $[17.1]^3\Pi_g - X^3\Sigma_u^+$ transition system (cm^{-1}).

State	v	T_0 (cm^{-1})	B_{eff} (cm^{-1})
$^3\Pi_g$	3	17 796.4(7)	0.0490(5)
	2	17 581.5(8)	0.0492(5)
	1	17 364.4(7)	0.0494(5)
	0	17 146.3(6)	0.0496(5)
$X^3\Sigma_u^+$	1	211.4(5)	0.0500(3)
	0	0	0.0515(3)

the upper state is an inverted $^3\Pi_g$ state. The vibrational band origins for the $[17.1]^3\Pi_g - X^3\Sigma_u^+$ transition system of Pd_2 are listed in Table I.

Since the recorded bands have well defined contour, we have attempted to simulate the band contour using the PGOPHER program.[34] The band contour was simulated using molecular constants for the upper and lower states with a temperature set at about 60 K and a linewidth of 0.12 cm^{-1}. A sub-program was written to incorporate contributions from all the 15 isotopic molecules that have slightly different molecular constants arising from the differences in reduced masses and their relative abundance. The overall simulated contour was compared to the experimentally observed envelope for determining the quality of the fit. At this stage, only molecular constants for both the upper and lower states were adjusted until an acceptable fit was obtained. Figure 3 shows the simulation results of the (1, 0) band of the $^3\Pi_{1g} - {}^3\Sigma_{0u^-}^+$ and $^3\Pi_{2g} - {}^3\Sigma_{1u}^+$ sub-band transitions and the observed spectrum. The solid black line is the observed spectrum and the dash lines are the simulation results. The broad features of the simulated contour matched reasonably well with the observed contour although there was some slight discrepancy in reproducing the fine features. Considering the complexity of this simulation process, the agreement is quite reasonable. The molecular constants used in the fit are listed in Table II. From the simulation results, the bond length r_0 determined for the excited $^3\Pi_g$ state and the ground $X^3\Sigma_u^+$ state are 2.52(4) Å and 2.47(4) Å, respectively. Since only the band contour was fitted, the obtained bond lengths should only be

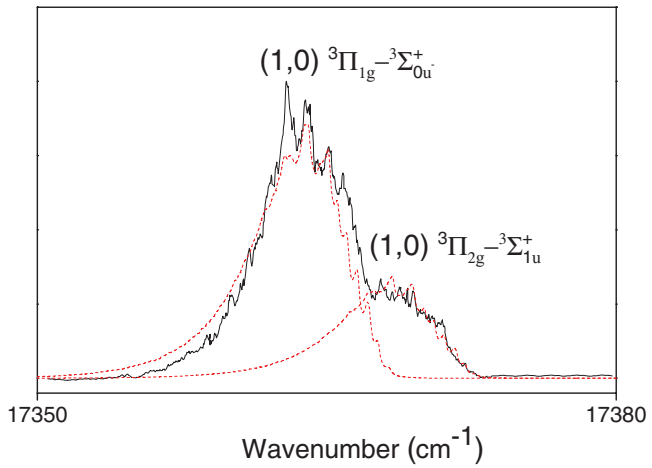

FIG. 3. Simulated and experimental band contour fit of the (1, 0) band of $^3\Pi_{1g} - {}^3\Sigma_{0u^-}^+$ and $^3\Pi_{2g} - {}^3\Sigma_{1u}^+$ sub-band transitions.

considered as approximate. This is why there is a relatively large uncertainty in these values.

For the ground $X^3\Sigma_u^+$ state, the $\Delta G_{1/2}$ was determined to be 211.4(5) cm^{-1}, which is of higher accuracy than the value obtained by Lineberger.[30,31] The ground $X^3\Sigma_u^+$ state is subjected to a sizable second-order spin-orbit coupling effect, which separates the $^3\Sigma_{0u^-}^+$ and the slightly higher energy $^3\Sigma_{1u}^+$ components. In a $^3\Pi_g - {}^3\Sigma_u^+$ transition, the $^3\Pi_{1g} - {}^3\Sigma_{0u^-}^+$ sub-band is the only sub-band that can originate from the $^3\Sigma_{0u^-}^+$ sub-state. The other two sub-bands, $^3\Pi_{2g} - {}^3\Sigma_{1u}^+$ and $^3\Pi_{0g} - {}^3\Sigma_{1u}^+$ originate from the $^3\Sigma_{1u}^+$ sub-state. When the beam of molecules is cold enough that only the ground sub-state is well-populated, one strong sub-band is expected if the $^3\Sigma_{0u^-}^+$ sub-state lies lower in energy, while two strong sub-band systems are expected if the $^3\Sigma_{1u}^+$ sub-state lies lower in energy. Thus, the fact that we observe one strong sub-band system and two-very weak ones shows that the $^3\Sigma_{0u^-}^+$ sub-state lies lower than the $^3\Sigma_{1u}^+$ sub-state. Other than this fact, however, our data do not permit us to establish the magnitude of the spin-orbit splitting in either the $^3\Sigma_u^+$ or the $^3\Pi_g$ state.

As shown in Table I, the sub-bands identified are consistent with a $^3\Pi - {}^3\Sigma$ transition, but it is immediately clear that the spin structure of one of the electronic states must be unusual because the sub-bands do not lie in an expected energy order.[35] Generally, for a $^3\Pi$ state, the first order spin-orbit coupling gives rise to relatively large and roughly equal spin-orbit separations between the three spin components, and the spin-spin splitting of a $^3\Sigma$ state would normally be small. The expected pattern for a $^3\Pi - {}^3\Sigma$ transition would have approximately equally separated sub-band transitions and the $^3\Pi_{2g} - {}^3\Sigma_{1u}$ sub-band is of the highest energy. As far as the (0, 0) band is concerned, the $^3\Pi_{2g} - {}^3\Sigma_{1u}^+$ and the $^3\Pi_{1g} - {}^3\Sigma_{0u^-}^+$ sub-band transitions are fairly close to each other; if the ground state separation between the $^3\Sigma_{1u}^+$ and $^3\Sigma_{0u^-}^+$ components is small, the spin-orbit splitting between the $^3\Pi_{2g}$ and $^3\Pi_{1g}$ sub-states would also be abnormally small. As shown in Table I, the energy separation between the $^3\Pi_{2g}$ and $^3\Pi_{0g}$ sub-state is 82.0 cm^{-1}, it is unreasonable to have the energy separation for the $^3\Pi_{2g}$ and $^3\Pi_{1g}$ spin components to be only a few wavenumber for all the three observed vibrational levels. If the 32 cm^{-1} splitting indicated by Lineberger and coworkers[30,31] was taken to be the effective spin-spin separation of the ground state, the spin-orbit separation between the $^3\Pi_{2g}$ and $^3\Pi_{1g}$, and $^3\Pi_{1g}$ and $^3\Pi_{0g}$ sub-states are, respectively, 37 and 45 cm^{-1} for the v = 0 level, 36.5 and 61.2 cm^{-1} for the v = 1 level, and 32 and 64.7 cm^{-1} for the v = 2 level. The

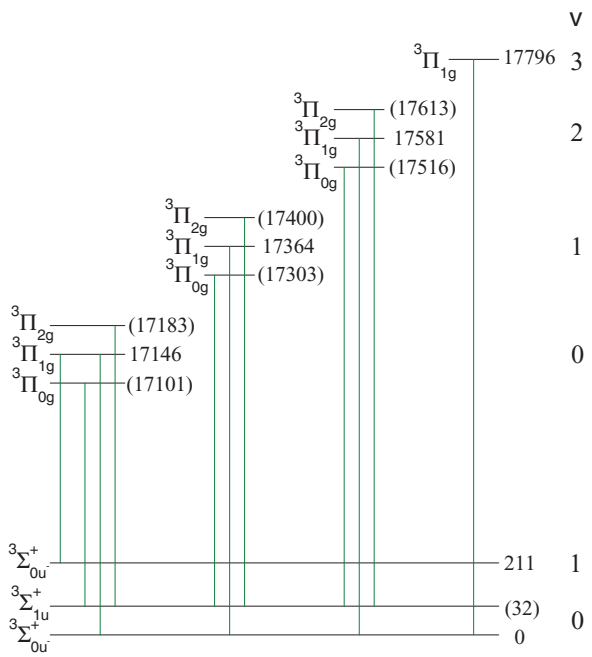

FIG. 4. Energy level diagram of the $[17.1]^3\Pi_g - X^3\Sigma_u^+$ transition of Pd_2 (Energy given in parenthesis is based on the assumption that the $^3\Sigma_{1u}^+$ v = 0 level lies 32 cm^{-1} above the $^3\Sigma_{0u^-}^+$ v = 0 level).

transition band observed and their corresponding assembled energy levels are given in Figure 4.

Figure 5 shows qualitatively the relative energy order of the MOs formed from the 4*d* and 5*s* atomic orbitals (AO) of the Pd atoms. The more stable $4d\sigma_g$, $4d\pi_u$, $4d\delta_g$ MOs and the higher energy $4d\sigma_u$, $4d\pi_g$, $4d\delta_u$ MOs are formed from the Pd $4d\sigma$, $4d\pi$ and $4d\delta$ AOs. The $5s\sigma_g$ and $5s\sigma_u$ MOs are formed from the Pd 5*s* AOs. The Pd_2 molecule has a $X^3\Sigma_u^+$ ground state, and the electronic configuration is

$$4d\sigma_g^2\,4d\pi_u^4\,4d\delta_g^4\,4d\delta_u^4\,4d\pi_g^4\,5s\sigma_g^1\,4d\sigma_u^1 \rightarrow X^3\Sigma_u^+ \text{ and } {}^1\Sigma_u^+. \quad (1)$$

From our observed spectrum, there is no doubt that the $X^3\Sigma_u^+$ state is the ground state of Pd_2 with electrons in the $\sigma_g^1\sigma_u^1$ configuration. Due to the spin-orbit coupling effects, the

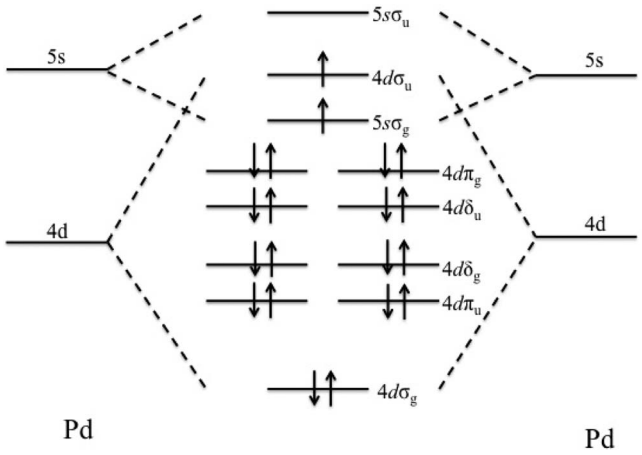

FIG. 5. Molecular orbital diagram for the valence orbitals for Pd_2. The electrons are arranged to show the ground state electronic configuration.

TABLE III. Bond length and vibrational frequency of the ground $X^3\Sigma_u^+$ state of Pd_2.

Authors	Method of determination	Symmetry	Bond length (Å)	Vib. freq. (cm^{-1})
SG[a]	*Ab inito* HF/CI	$^1\Sigma_g^+$	2.75	132
B[b]	CASSCF/MRSDCI + RCI	$^3\Sigma_u^+$ (1_u)	2.48	159
LBK[c]	LSD theory	$^3\Sigma_u^+$	2.44	222
SMMM[d]	CISC	$^3\Sigma_u^+$	2.49	227
EZ[e]	SCF/CI, MRCIS-INDO	$^3\Sigma_u^+$	2.46	...
HD[f]	Nonlocal DFT (ECP)	Triplet	2.53	195
EGS[g]	DFT/B3LYP (Basis I and II)	Triplet	2.76	206.6
HPEC[h]	Photo-detachment spectroscopy	$^3\Sigma_u^+$	...	210
This work	LIF spectroscopy	$^3\Sigma_u^+$	2.47	211.4

[a]Reference 11.
[b]References 13 and 14.
[c]Reference 15.
[d]Reference 16.
[e]Reference 17.
[f]Reference 19.
[g]Reference 23.
[h]References 30 and 31.

ground $X^3\Sigma_u^+$ state splits into two spin components: $X^3\Sigma_u^+$ (1_u) and $X^3\Sigma_u^+$ (0_u^-) and are designated as $^3\Sigma_{1u}^+$ and $^3\Sigma_{0u^-}^+$, respectively.

The available calculation results and experimental determinations of the ground state of Pd_2 molecule are summarized in Table III. Except Shim and Gingerich[11] and Efremenko *et al.*,[23] all other calculations were able to obtain the $X^3\Sigma_u^+$ ground state. However, the predicted bond length varied from case to case and there seemed to be fewer agreements on the calculated vibrational frequency.

It is enlightening and interesting to compare the electronic structure of both the Group VIIIA (nickel) and Group IB (coinage group) dimers. The corresponding ground state information is summarized in Table IV. The coinage group dimers are most well studied molecules due to a large variety of production methods and the simple closed *d*-shell configuration in the atomic ground state.[36–43] Extensive investigations on Ni_2 and Pt_2 have also been reported both experimentally and theoretically.[31,44–52] For the transition metals, it is generally recognized that the size of the n*d* and (n+1)*s* orbitals change as one moves across the periodic table from left to right: the n*d* orbitals contract more heavily than the (n+1)*s* orbital. Therefore, *d* orbitals in the late transition metals are less available for chemical bonding. Unlike the 3*d* series, this effect is less severe in the 4*d* and 5*d* series where the relativistic effect causes *s* orbital contraction and *d* orbital expansion.

Nickel as a 3*d* metal has a $3d^84s^2(^3F_4)$ atomic ground state. In order to engage in an effective chemical bonding, both atoms are required to be excited to the $3d^94s^1(^3D_3)$ configuration. Note that this requires only 204.787 cm^{-1} of energy per Ni atom, an amount that is negligible compared to the strength of the Ni-Ni bond. Morse *et al.*[46] performed ligand field calculation and conducted experimental investigations[44,47] on the nickel dimer (Ni_2), the most recent

TABLE IV. Spectroscopic properties of the ground state of Group VIIIA and IB dimer.

	Symmetry	r_0 (Å)	ω_e (cm^{-1})
Ni_2[a]	0_u^- or 0_g^+	2.1545	280[b]
Pd_2[c]	$^3\Sigma_u^+$	2.47	211.4[d]
Pt_2[e]	$^3\Sigma_g^-$	2.3330	222.46
Cu_2[f]	$^1\Sigma_g^+$	2.2197	226.43
Ag_2[g]	$^1\Sigma_g^+$	2.5303	192.4
Au_2[h]	$^1\Sigma_g^+$	2.4719	190.176

[a]Reference 47.
[b]Reference 31.
[c]This work.
[d]$\Delta G_{1/2}$.
[e]References 50 and 51.
[f]Reference 40.
[g]Reference 42.
[h]Reference 36.

results agree with their prediction that the 3*d* hole is localized in the *dδ* orbital. It suggests that the *d* orbitals of two nickel atoms are only weakly interacting with each other and it is mainly 4*s* orbitals that form the chemical bond. The ground state of Ni_2 was determined to be either 0_u^- or 0_g^+. Although Ni_2 and Cu_2 have virtually identical bond energies, the bond length of Ni_2 is somewhat shorter than that of Cu_2. It has been suggested by Morse[47] that this may be due to contributions of ionic states such as $d_A^8 d_B^{10}\sigma_g^2$ (Ni^+Ni^-) and $d_A^{10} d_B^8\sigma_g^2$ (Ni^-Ni^+) to the ground state wavefunction. No analogous states are possible in Cu_2.

The platinum dimer (Pt_2) is constructed with the two Pt atoms in $5d^96s^1(^3D_3)$ state and the Pt_2 ground state is determined to be either 0_u^- or 0_g^+.[50] Early calculations predicted two *dδ* holes in the ground state electronic configuration,[45] but the large bond energy found experimentally suggestions that the d-holes are located in orbitals that are more strongly anti-bonding than the $5d\delta_u$ orbitals. By making comparison with Au_2, Morse claimed that the *d* orbitals contribute substantially to the bonding, leading to a strong Pt-Pt bond equivalent to a double bond. Recently, O'Brien *et al.*[51] suggest that the 5d-holes are located in the $5d\pi_g$ anti-bonding orbitals leading Pt_2 to have a $^3\Sigma_g^-$ ground state with a double bond.

For Pd_2, the Hartree-Fock calculations performed by Gingerich and co-workers[11] showed that the interaction between the two Pd atoms in their $4d^{10}$ ($^1S_0$) ground state is essentially repulsive and that excitation to $4d^95s^1$ ($^3D_3$) is needed to form a chemical bond. They predicted the ground state to be $^1\Sigma_g^+$ from the combination of two excited state atoms in their $4d^95s^1$ ($^3D_3$) states. They assumed that among the holes in localized *dσ*, *dπ*, *dδ* orbitals, the configuration with the holes in the 4*dδ* orbitals resulted in the lowest total energy. The *ab inito* calculations by Balasubramanian[13] suggested a $^3\Sigma_u^+$ ground state for Pd_2 from bringing together one atom in the $4d^{10}$ ($^1S_0$) state and one excited atom in the $4d^95s^1$ ($^3D_3$) state. This new approach resulted in the ground state that agreed with the photo-detachment experiment[31] and our results. Their assignment of the MO valence configuration is shown in Figure 5.

In conclusion, the LIF spectrum exhibits a pattern of $^3\Pi_g - {}^3\Sigma_u^+$ transition and the vibrational structure allowed the determination of the vibrational frequency of both the ground and excited states. Using the method of contour simulation, the rotational constants and, hence, the bond length of the two states involved were estimated. In our analysis, the intensity of transitions involving the $X^3\Sigma_u^+(0_u^-)$ sub-state is always the strongest and also consistent with the assignment of it to be the lowest energy component of the ground state. With the help of a simple molecular orbital argument, we examined the bonding characteristics of the 4*d* and 5*s* orbitals of the Pd_2 molecule.

ACKNOWLEDGMENTS

The work described here was supported by a grant from the Research Grants Council of the Hong Kong Special Administrative Region, China (Project No. HKU 701008). Zhihua Chen would like to thank the Faculty of Science of the University of Hong Kong for the Summer Research Fellowship. We would like to thank Professor Colin Western (University of Bristol, UK) for permissions to use the PGOPHER software and the reviewers for suggestions to improve the paper.

[1]H. B. Li, S. Johansson, C. C. Carin, and T. J. Colacot, ACS Catal. **2**, 1147 (2012).
[2]D. Astruc, Inorg. Chem. **46**, 1884 (2007).
[3]O. Savadogo, K. Lee, K. Oishi, S. Mitsushima, N. Kamiya, and K. I. Ota, Electrochem. Commun. **6**, 105 (2004).
[4]S. L. Buchwald, Acc. Chem. Res. **41**, 1439 (2008).
[5]R. S. DaBell, R. G. Meyer, and M. D. Morse, J. Chem. Phys. **114**, 2938 (2001).
[6]J. D. Langenberg, L. Shao, and M. D. Morse, J. Chem. Phys. **111**, 4077 (1999).
[7]T. M. Ramond, G. E. Davico, F. Hellberg, F. Svedberg, P. Salén, P. Söderqvist, and W. C. Lineberger, J. Mol. Spectrosc. **216**, 1 (2002).
[8]Y. W. Ng, H. F. Pang, Y. Qian, and A. S. C. Cheung, J. Phys. Chem. A **116**, 11568 (2012).
[9]K. A. Gingerich, Naturwissenschaften **54**, 43 (1967).
[10]J. W. Weltner and R. J. V. Zee, Ann. Rev. Phys. Chem. **35**, 291 (1984).
[11]I. Shim and K. A. Gingerich, J. Chem. Phys. **80**, 5107 (1984).
[12]M. D. Morse, Chem. Rev. **86**, 1049 (1986).
[13]K. Balasubramanian, J. Chem. Phys. **89**, 6310 (1988).
[14]K. Balasubramanian, J. Phys. Chem. **93**, 6585 (1989).
[15]S. Lee, D. Bylander, and L. Kleinman, Phys. Rev. B **39**, 4916 (1989).
[16]P. Schwerdtfeger, J. S. McFeaters, J. J. Moore, and D. M. McPherson, Langmuir **7**, 116 (1991).
[17]G. L. Estiu and M. C. Zerner, J. Phys. Chem. **98**, 4793 (1994).
[18]A. Goursot, I. Papai, and C. A. Daul, Int. J. Quantum Chem. **52**, 799 (1994).
[19]M. Harada and H. Dexpert, J. Phys. Chem. **100**, 565 (1996).
[20]G. Valerio and H. Toulhoat, J. Phys. Chem. **100**, 10827 (1996).
[21]J. M. Seminario, A. G. Zacarias, and M. Castro, Int. J. Quantum Chem. **61**, 515 (1997).
[22]V. Bertani, C. Cavallotti, M. Masi, and S. Carra, J. Phys. Chem. A **104**, 11390 (2000).
[23]I. Efremenko, E. D. German, and M. Sheintuch, J. Phys. Chem. A **104**, 8089 (2000).
[24]E. Cances, J. Chem. Phys. **114**, 10616 (2001).
[25]M. Moseler, H. Hakkinen, R. N. Barnett, and U. Landman, Phys. Rev. Lett. **86**, 2545 (2001).
[26]J. R. Lombardi and B. Davis, Chem. Rev. **102**, 2431 (2002).
[27]Z. J. Wu, Chem. Phys. Lett. **383**, 251 (2004).
[28]W. E. Klotzbuecher and G. A. Ozin, Inorg. Chem. **19**, 3767 (1980).
[29]S. Taylor, E. M. Spain, and M. D. Morse, J. Chem. Phys. **92**, 2710 (1990).
[30]J. Ho, K. M. Ervin, M. L. Polak, M. K. Gilles, and W. C. Lineberger, J. Chem. Phys. **95**, 4845 (1991).
[31]J. Ho, M. L. Polak, K. M. Ervin, and W. C. Lineberger, J. Chem. Phys. **99**, 8542 (1993).
[32]Y. W. Ng, H. F. Pang, and A. S. C. Cheung, J. Chem. Phys. **135**, 204308 (2011).
[33]Q. Ran, W. S. Tam, C. S. Ma, and A. S. C. Cheung, J. Mol. Spectrosc. **198**, 175 (1999).

[34]M. E. Green and C. M. Western, J. Chem. Phys. **104**, 848 (1996).
[35]G. Herzberg, *Molecular Spectra and Molecular Structure: Spectra of Diatomic Molecules* (Krieger Publishing Company, Malabar, 1989).
[36]L. L. Ames and R. F. Barrow, Trans. Faraday Soc. **63**, 39 (1967).
[37]C. M. Brown and M. L. Ginter, J. Mol. Spectrosc. **69**, 25 (1978).
[38]D. R. Preuss, S. A. Pace, and J. L. Gole, J. Chem. Phys. **71**, 3553 (1979).
[39]D. E. Powers, S. G. Hansen, M. E. Geusic, A. C. Pulu, J. B. Hopkins, T. G. Dietz, M. A. Duncan, P. R. R. Langridge-Smith, and R. E. Smalley, J. Phys. Chem. **86**, 2556 (1982).
[40]E. A. Rohlfing and J. J. Valentini, J. Chem. Phys. **84**, 6560 (1986).
[41]B. Simard and P. A. Hackett, J. Mol. Spectrosc. **142**, 310 (1990).
[42]V. Beutel, H. G. Krämer, G. L. Bhale, M. Kuhn, K. Weyers, and W. Demtröder, J. Chem. Phys. **98**, 2699 (1993).
[43]A. M. James, P. Kowalczyk, B. Simard, J. C. Pinegar, and M. D. Morse, J. Mol. Spectrosc. **168**, 248 (1994).
[44]M. D. Morse, G. P. Hansen, P. R. R. Langridge-Smith, L. S. Zheng, M. E. Geusic, D. L. Michalopoulos, and R. E. Smalley, J. Chem. Phys. **80**, 5400 (1984).
[45]K. Balasubramanian, J. Chem. Phys. **87**, 6573 (1987).
[46]E. M. Spain and M. D. Morse, J. Chem. Phys. **97**, 4641 (1992).
[47]J. C. Pinegar, J. D. Langenberg, C. A. Arrington, E. M. Spain, and M. D. Morse, J. Chem. Phys. **102**, 666 (1995).
[48]C. J. Barden, J. C. Rienstra-Kiracofe, and F. Schaefer III, J. Chem. Phys. **113**, 690 (2000).
[49]J. C. Fabbi, J. D. Langenberg, Q. D. Costello, M. D. Morse, and L. Karlsson, J. Chem. Phys. **115**, 7543 (2001).
[50]M. B. Airola and M. D. Morse, J. Chem. Phys. **116**, 1313 (2002).
[51]L. C. O'Brien and J. J. O'Brien, J. Chem. Phys. **134**, 184304 (2011).
[52]A. V. Cheskidov, A. A. Buchachenko, and D. S. Bezrukov, J. Chem. Phys. **136**, 214304 (2012).